Available online at www.sciencedirect.com
SCIENCE DIRECT
Carbohydrate Research 341 (2006) 1848–1858
Carbohydrate RESEARCH

Low- and high-resolution nuclear magnetic resonance (NMR) characterisation of hyaluronan-based native and sulfated hydrogels

Rolando Barbucci,[a,*] Gemma Leone,[a] Antonio Chiumiento,[a] Maria Enrica Di Cocco,[b] Giovanni D'Orazio,[b] Raffaella Gianferri[b] and Maurizio Delfini[b]

[a]*CRISMA and Department of Chemical and Biosystem Sciences and Technologies, University of Siena, Via Aldo Moro 2, 53100 Siena, Italy*
[b]*Department of Chemistry, 'La Sapienza' University, Piazzale Aldo Moro 5, 00185 Roma, Italy*

Received 24 January 2006; received in revised form 7 April 2006; accepted 15 April 2006
Available online 22 May 2006

Abstract—Hyaluronan-based hydrogels were synthesised using different crosslinking agents, such as 1,3-diaminopropane (1,3-DAP) and 1,6-diaminohexane (1,6-DAE). The hydrogels were sulfated to provide materials (Hyal-1,3-DAP, Hyal-1,6-DAE, HyalS-1,3-DAP and HyalS-1,6-DAE) that were characterised by both high- and low-resolution nuclear magnetic resonance (NMR) spectroscopy. The ^{13}C NMR spectra of the materials were analysed to identify, characterise and study the crosslinking degree of the hydrogels. The crosslinking degree was also determined by potentiometric titration and the effectiveness of the two techniques was compared. Measurements of longitudinal relaxation times (spin–lattice) and of NOE enhancement were used to study the mobility of the hydrogels. Low-resolution NMR studies allowed the determination of the water transport properties in the hydrogels. In addition, the swelling degree for the various hydrogels was calculated as a function of the longitudinal and transversal relaxation times of the water molecules. Lastly, the self-diffusion coefficients of the water in interaction with the four polysaccharides were measured by the pulsed field gradient spin echo (PFGSE) sequence.

Keywords: Hyaluronan; Hydrogel; NMR characterisation

1. Introduction

A topic currently of interest in materials science is the development of 'intelligent' materials or structures that are able to undergo structural changes in response to environmental modifications.[1] A material can be considered an intelligent one if it possesses a sensor and an effector function. The sensor function is generally played by substances and/or ions, included or being part of the system, that are able to perceive the environmental stimulus, whereas the effector function is played by the material, which structurally changes itself in response to the stimulus and afterwards it is able to perform a specific biological function.[2]

Among the several classes of stimuli-sensitive materials, hydrogels are the most analysed and studied systems.[3] Hydrogels can be defined as physically or chemically crosslinked polymer chains that are able to absorb a great amount of fluid.[4] The swelling properties, or the swelling kinetics and the maximum amount of adsorbed fluid (water up-take), are affected by several factors such as temperature, light, electrical voltage, pH and salt concentration.[5–7] Consequently, hydrogels, undergoing volume changes in response to environmental stimuli, can be described as intelligent-materials. The presence of positive or negative charges in the polymeric chains (polyelectrolyte polymers) guarantees a significant and rapid response to environmental changes.

* Corresponding author. Tel.: +39 577 234382; fax: +39 577 234383; e-mail: barbucci@unisi.it

0008-6215/$ - see front matter © 2006 Published by Elsevier Ltd.
doi:10.1016/j.carres.2006.04.046

There are several classes of natural polyelectrolytes that can be used as starting polymers to obtain hydrogels. Among these, polysaccharides are useful because they show a high number of charges and a high aptitude for having their chemical composition modified by the introduction of new functional groups, such as amide, sulfate or carboxylate groups.

Hyaluronic acid (Hyal) is one of the most analysed and studied polysaccharides. It is a natural linear polysaccharide with a repeating disaccharide unit consisting of 2-acetamido-2-deoxy-β-D-glucopyranose and β-D-glucopyranuronic acid residues linked alternatingly by (1→3) and (1→4) glycosidic bonding. Hyal is a weak polyacid with a very low charge density because only one charge is present for each repeating disaccharidic unit. Nevertheless, due to the ease with which its chemical composition can be modified, different charged functional groups, such as sulfate groups, can be introduced.[8,9] This capability and their morphology, which is very similar to that of human tissues, open up possibilities for the use of hydrogels in the biomedical field.[10–12] In fact, as hydrogels are able to absorb a large amount of aqueous fluids, they take on a soft and open structure that permits the allocation of cells, their adhesion and proliferation, that is, biocompatibility. Another consequence of the very high amount of water absorbed is the high performance of these materials as lubricants.[13] In fact, the high water content decreases friction and makes these hydrogels suitable as coatings. Finally, hyaluronan-based hydrogels can be used as fillers in plastic surgery.[14] Nowadays, several hyaluronan-based commercial preparations are present in the world market, especially physical hydrogels or very highly viscous solutions. Hylaform and Restylane,[15] for example, are fairly new dermal fillers, which are both FDA-approved for the treatment of wrinkles. Hylaform is derived from a highly purified form of hyaluronic acid, which is a natural substance found in human skin, while Restylane is derived from a biodegradable non-animal stabilised hyaluronic acid (NASHA™). The major disadvantages of these commercial preparations are their low stability and fast degradability, which make frequent injections necessary. A chemically crosslinked hydrogel may represent a solution. In fact, the presence of covalent bonds induces a greater stability, resulting in a longer time for a complete degradation of the system and reduced frequency of the surgical treatments.

In this work, thixotropic hyaluronan-based 50% hydrogels (i.e., 50% of the carboxylic groups of the polysaccharide chains that are involved in the crosslinking reaction) were synthesised and studied using different alkylic diamines, such as 1,3-diaminopropane (DAP) and 1,6-diaminohexane (DAE), as the crosslinking agents.[16,17] Hyaluronan hydrogels were sulfated to introduce new charged functional groups capable of increasing the biocompatibility and the swelling properties consequently expanding their biomedical applications. A ^{13}C high-resolution NMR study was carried out to evaluate the structure, the degree of crosslinking and the motional properties. The interaction of the fluid medium water with the polymeric matrices was investigated by NMR relaxation times at low resolution. The sulfation reaction was checked by IR analysis and the sulfation degree was also evaluated.

2. Results and discussion

2.1. Hydrogel synthesis and characterisation

The hydrogel synthesis was carried out with the polysaccharide in the form of a tetra-*n*-butylammonium (TBA) salt, in DMF solution under nitrogen flow. This was necessary to guarantee an anhydrous environment, because the polymer in the TBA form is a highly hygroscopic substance and a high amount of humidity could alter the synthetic process. The temperature control (4 °C) was necessary because the activating used, 2-chloro-1-methylpyridinium iodide (CMP-I), induces the formation of hydrophobic interactions at a higher temperature, favouring the formation of a physical hydrogel. This phenomenon produced a heterogeneous mixture and hindered the crosslinking process. The CMP-I was added in a stoichiometric amount, depending on the amount of carboxylate groups to be activated (in this case 50% of the carboxylic groups of the polysaccharide chain). Activation of the polysaccharide carboxylate groups took place rapidly by a nucleophilic attack on the carboxylate group by CMP-I and the liberation of tetra-*n*-butylammonium chloride. The intermediate then underwent a nucleophilic attack on the carboxylic group by the alkylic diamine, with the elimination of the heterocyclic compound in the form of 1-methyl-2-pyridone. The reaction was catalysed by a small amount of triethylamine as a hydrogen iodide scavenger. The product of the reaction took on the characteristics of a hydrogel, even in organic solvent.[18] Because the colorimetric ninhydrin assay was not able to detect free NH_2 groups, but their presence was highlighted by the more sensitive NMR analysis, it can be stated that the amount of free NH_2 groups was negligible (under the ninhydrin assay detection limit of $<10^{-3}$ M).

The sulfation reaction was performed on the already crosslinked hydrogels and a superficial distribution of sulfate groups was consequently obtained (Fig. 1).

A different sulfation degree was obtained for Hyal-1,3-DAP and Hyal-1,6-DAE. In fact, 5.4 $(\pm 1.0) \times 10^{-6}$ and 1.0 $(\pm 0.5) \times 10^{-6}$ mol of sulfate groups per mg of dry hydrogels were found, respectively. Furthermore, the sulfation reaction was checked by FT-IR analysis. Figure 2 shows the FT-IR spectra of HyalS-1,3-DAP compared with that of Hyal-1,3-DAP. The most

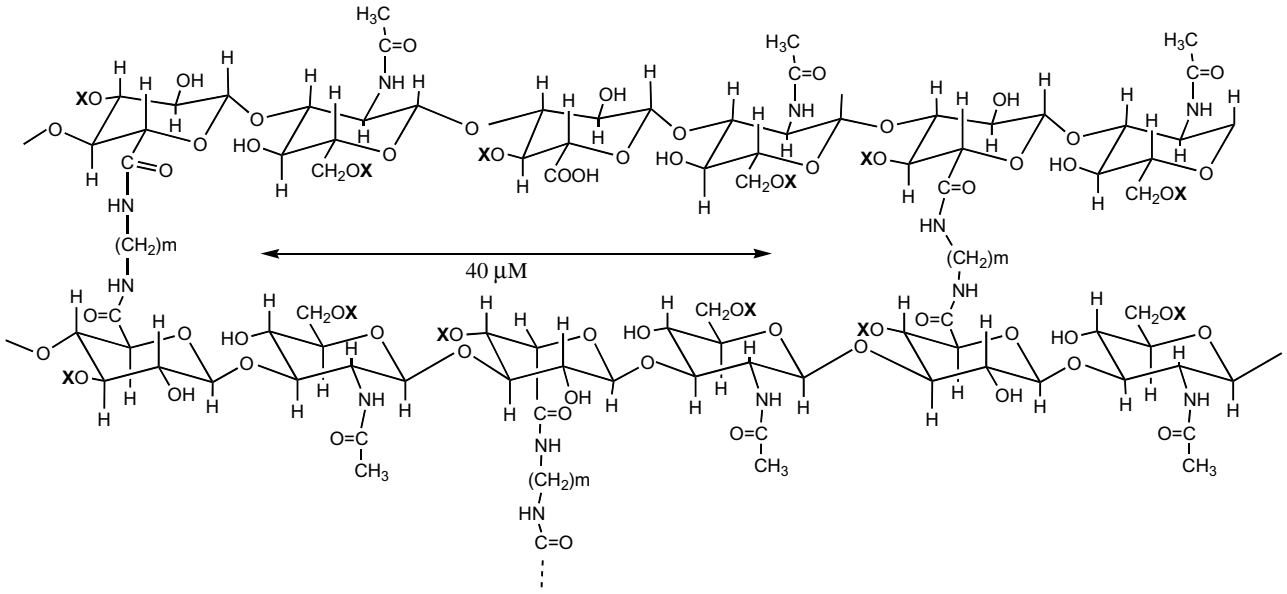

Figure 1. Schematic representation of the homogeneous structure of hydrogels with reproducible meshes (≅40 μm) for all the hydrogels. X = H or OSO3–; *m* = 3: 1,3-DAP; *m* = 6:1,6-DAE.

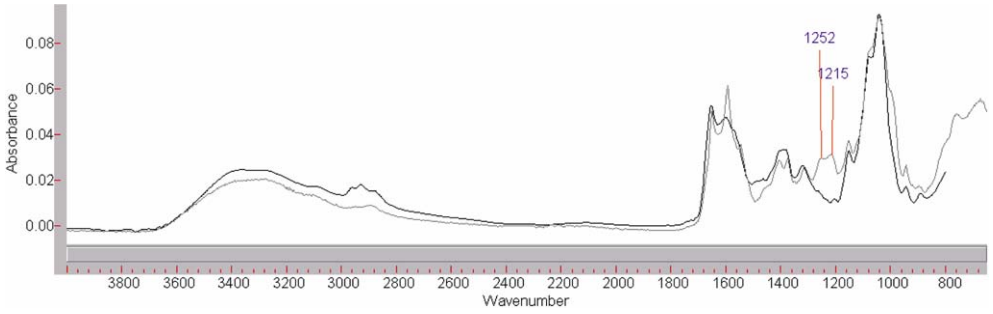

Figure 2. IR spectra of Native Hyal-1,3-DAP (black) and HyalS-1,3-DAP (grey).

significant difference is a double peak in the 1250 cm^{-1} region, which is attributed to the S=O stretching.[19] The presence of that peak confirmed the hydrogel sulfation. A similar result was found comparing the IR spectra of Hyal-1,6-DAE and HyalS-1,6-DAE.

2.2. Hydrogel structure study

Spectral features of the hydrogels examined seem to be identical with those of Hyal solutions, although the ^{13}C peaks of the hydrogels are slightly broadened. Nevertheless, comparing the spectra of the hydrogels with those of Hyal aqueous solutions, no chemical shift displacements were observed. ^{13}C NMR spectroscopy was used to characterise the structure of the four hydrogels examined. ^{13}C spectra of the crosslinked non-sulfated hydrogels are reported in Figures 3A and B and 4.

The peaks in the spectra were assigned on the basis of literature data,[20–22] by DEPT and by Gated decoupling techniques. The assignments, longitudinal relaxation times (T_1), NOE (η) and half-height linewidth of signals ($\Delta\nu_{1/2}$) of selected signals are reported in Tables 1–4 for all examined hydrogels.

In the carbonyl region, the lower field signal was assigned to the carbonyl of the *N*-acetyl glucosamine unit (GlcNAc), which is specific to the non-crosslinked hyaluronan, and the higher field signal was assigned to the carbonyl of the glucuronic unit (GlcA). The signal at ~170 ppm was assigned to the carboxylate condensed with the diamine. The signals of the crosslinking agent, exhibiting chemical shifts between 25 and 40 ppm, are present in the spectra. Moreover, weak signals between 110 and 155 ppm are present, arising from aromatic systems belonging to the activating agent (CMP-I) and to impurities in the native hyaluronic acid. The resonances at ~38 ppm can be attributed to the carbons C1 and C3 of the crosslinked and non-crosslinked 1,3-diaminopropane, respectively, whereas the resonances at ~25 ppm are attributed to the carbons C2 of the crosslinked and non-crosslinked 1,3-diaminopropane, respectively.

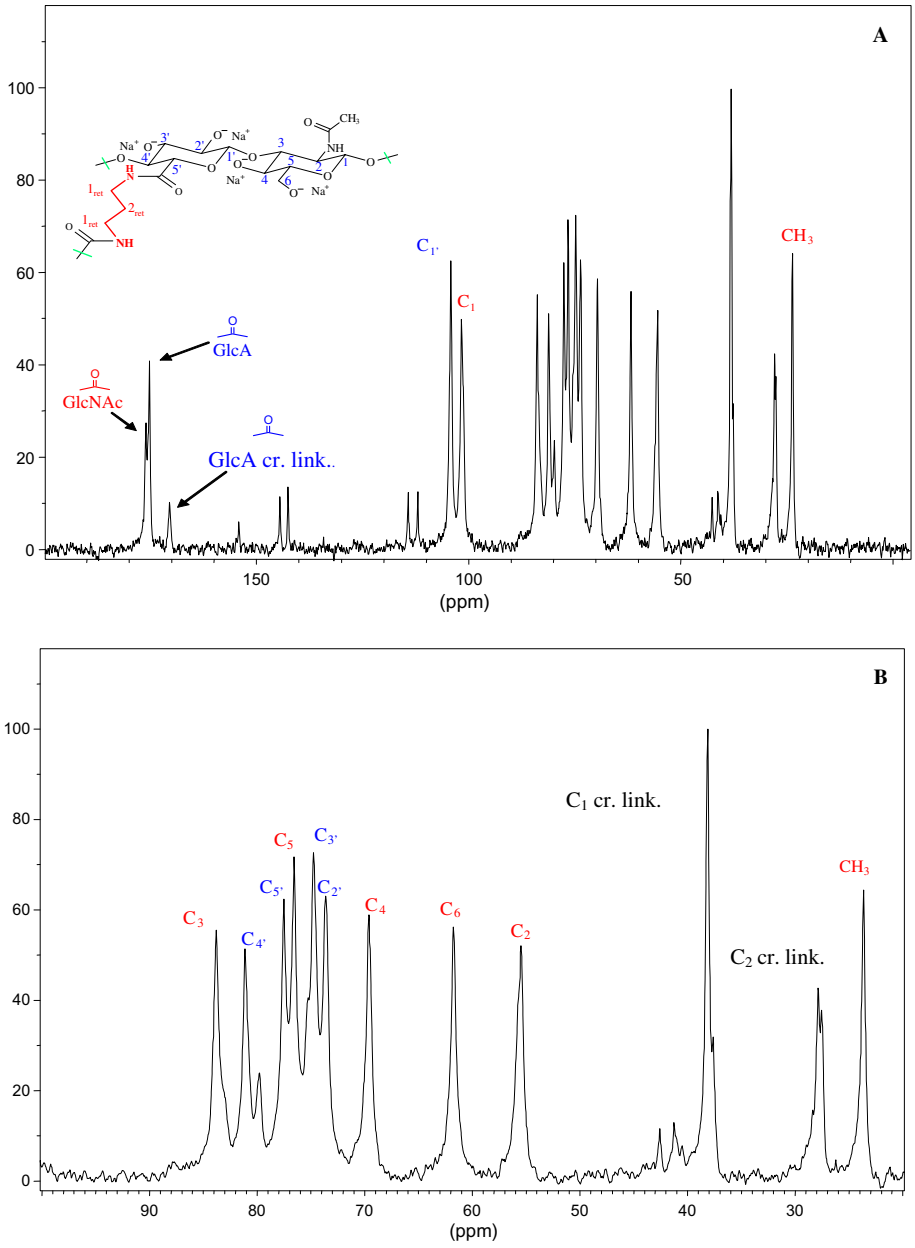

Figure 3. (A) ^{13}C NMR spectrum of Hyal-1,3-DAP. The spectrum was recorded on hydrogels swollen in deuterium oxide at the controlled temperature of 310 ± 1 K. (B) Detail of (A); GlcNAc: *N*-acetyl glucosamine carbonyl; GlcA: glucuronic acid carbonyl.

Assignments of Hyal-1,6 crosslinked carbon resonances were made on the basis of the comparison with the Hyal-1,3 crosslinked polymers. Finally, in the case of the HyalS-1,6-DAP and the HyalS-1,6-DAE, the spectrum is basically the same as that of its non-sulfated homologue. Differences are exhibited by half-height signal width.

2.3. Degree of crosslinking

The degree of crosslinking was obtained by comparing the C═O (GlcA) and C═$O_{cr.link.}$ (GlcA) areas. The area of the glucuronic unit was obtained by performing a deconvolution of the experimental Lorentzian[23] from the carbonyl signal of the GlcNAc unit. The crosslinking degree was also evaluated by potentiometric titration. The crosslinking degree of native and sulfated hydrogels was almost identical (Table 5) as the sulfation was performed on already crosslinked Hyal-1,3-DAP and Hyal-1,6-DAE.

As shown in Table 5, similar results were obtained using the two different techniques to detect the degree of crosslinking. Moreover, both the NMR and the potentiometric results were close to the theoretical result, that is, to that obtainable from the amount of CMP-I added to the solution to activate 50% of the

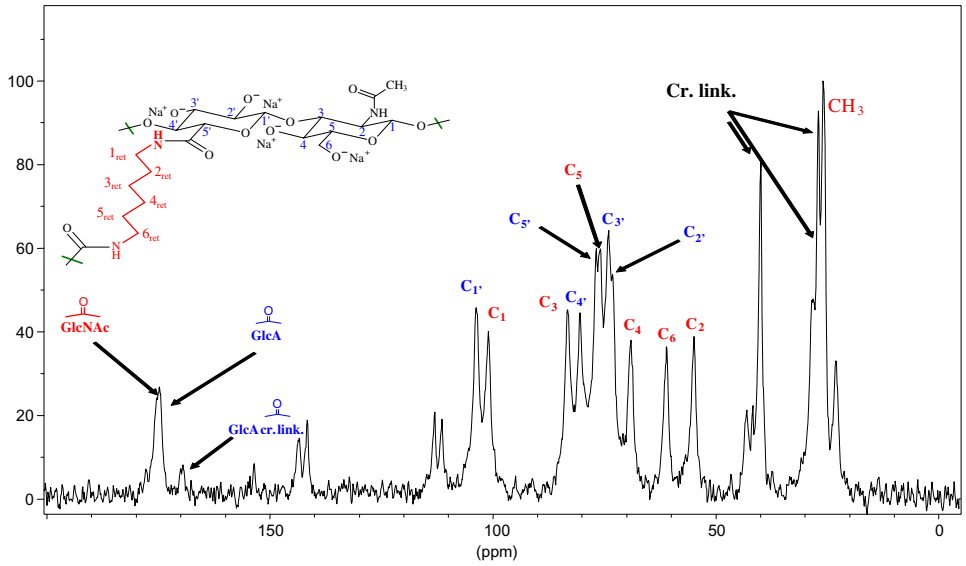

Figure 4. ^{13}C NMR spectrum of Hyal-1,6-DAE. The spectrum was recorded on hydrogels swollen in deuterium oxide at the controlled temperature of 310 ± 1 K.

Table 1. Assignments, longitudinal relaxation times (T_1), NOE (η) and half-height linewidth of signals ($\Delta\nu_{1/2}$) of selected signals for Hyal-1,3-DAP[a]

δ (ppm)	Assignment	T_1 (s)	η	$\Delta\nu_{1/2}$ (Hz)
176.02	C=O (GlcNAc)	2.800	0.7	44.21
175.20	C=O (GlcA)	3.710	0.7	39.30
170.50	$C{=}O_{cr.link.}$ (GlcA)	1.720	0.7	72.34
104.24	$C_{1'}$ (GlcA)	0.051	1.7	77.64
101.61	C_1 (GlcNAc)	0.056	1.8	70.74
83.78	C_3 (GlcNAc)	0.053	1.7	74.90
81.09	$C_{4'}$ (GlcA)	0.054	1.7	60.63
77.50	$C_{5'}$ (GlcA)	0.059	1.6	38.77
76.54	C_5 (GlcNAc)	0.064	1.7	45.80
74.74	$C_{3'}$ (GlcA)	0.057	1.8	61.10
73.63	$C_{2'}$ (GlcA)	0.064	1.7	43.48
69.59	C_4 (GlcNAc)	0.049	1.6	72.02
61.72	C_6 (GlcNAc)	0.058	1.7	43.90
55.44	C_2 (GlcNAc)	0.058	1.8	51.09

[a] Errors in the relaxation times are less than 5%.

Table 2. Assignments, longitudinal relaxation times (T_1), NOE (η) and half-height linewidth of signals ($\Delta\nu_{1/2}$) of selected signals for HyalS-1,6-DAP[a]

δ (ppm)	Assignment	T_1 (s)	η	$\Delta\nu_{1/2}$ (Hz)
175.76	C=O (GlcNAc)	2.680	0.7	42.90
175.23	C=O (GlcA)	3.540	0.7	38.63
170.54	$C{=}O_{cr.link.}$(GlcA)	1.915	0.7	71.85
104.24	$C_{1'}$ (GlcA)	0.049	1.7	98.55
101.61	C_1 (GlcNAc)	0.047	1.6	95.30
83.82	C_3 (GlcNAc)	0.060	1.7	80.58
81.12	$C_{4'}$ (GlcA)	0.052	1.7	71.53
77.48	$C_{5'}$ (GlcA)	0.060	1.7	46.00
76.57	C_5 (GlcNAc)	0.062	1.7	44.09
74.70	$C_{3'}$ (GlcA)	0.052	1.6	73.68
73.63	$C_{2'}$ (GlcA)	0.063	1.7	71.69
69.62	C_4 (GlcNAc)	0.050	1.7	107.54
61.72	C_6 (GlcNAc)	0.054	1.7	51.09
55.50	C_2 (GlcNAc)	0.052	1.7	53.23

[a] Errors in the relaxation times are less than 5%.

carboxylic groups present in the polysaccharide chain. In fact, as reported in Experimental, the activating agent was added in a sufficient quantity to activate 50% of the carboxylic groups. All these agreements allow us to state that the procedure used permits a strict control of the crosslinking degree.

2.4. Motional parameters

The ^{13}C NMR T_1, NOE and $\Delta\nu_{1/2}$, at 310 K are reported in Tables 1–4. T_2 was determined by the linewidth $\Delta\nu_{1/2}$ assuming a Lorentzian line shape:

$$\Delta\nu_{1/2} = 1/\pi T_2$$

T_1 and T_2 are of the same order as other crosslinked polymers.[24] Differences between T_1 and T_2 values are observed as polymeric molecules perform anisotropic motions rather than isotropic tumbling.[25] In particular, T_2 values derived from $\Delta\nu_{1/2}$ are more than one order of magnitude smaller than T_1.

The sulfated and non-sulfated crosslinked hyaluronans show well-resolved resonances. On the other hand, T_1 carbon atom values are lower than the values exhibited by non-crosslinked polymers. In fact, the T_1 values of our crosslinked hyaluronans are about tens of milliseconds while the non-crosslinked ones show values of about hundreds of milliseconds.[26] Such differences cannot be ascribed to the molecular weight of the polymers. In fact, the T_1 values of oligomers with different numbers of repeating units are very close to those of linear polymers.[27] The lower T_1 values can therefore be ascribed to the high crosslinking degree, which induces

Table 3. Assignments, longitudinal relaxation times (T_1), NOE (η) and half-height linewidth of signals ($\Delta\nu_{1/2}$) of selected signals for Hyal-1,6-DAE[a]

δ (ppm)	Assignment	T_1 (s)	η	$\Delta\nu_{1/2}$ (Hz)
178.55	C=O (GlcNAc)	2.850	0.7	20.80
176.06	C=O (GlcA)	3.800	0.7	28.42
175.50	$C{=}O_{cr.link.}$ (GlcA)	1.820	0.7	44.21
104.24	$C_{1'}$ (GlcA)	0.064	1.8	44.83
101.61	C_1 (GlcNAc)	0.060	1.7	46.13
83.82	C_3 (GlcNAc)	0.063	1.7	52.18
81.12	$C_{4'}$ (GlcA)	0.057	1.6	38.82
77.48	$C_{5'}$ (GlcA)	0.073	1.6	31.21
76.57	C_5 (GlcNAc)	0.086	1.8	30.90
74.70	$C_{3'}$ (GlcA)	0.069	1.9	34.23
73.63	$C_{2'}$ (GlcA)	0.077	1.8	28.42
69.62	C_4 (GlcNAc)	0.055	1.7	32.15
61.72	C_6 (GlcNAc)	0.059	1.6	29.20
55.50	C_2 (GlcNAc)	0.058	1.7	35.77

[a] Errors in the relaxation times are less than 5%.

Table 4. Assignments, longitudinal relaxation times (T_1), NOE (η) and half-height linewidth of signals ($\Delta\nu_{1/2}$) of selected signals for HyalS-1,6-DAE[a]

δ (ppm)	Assignment	T_1 (s)	η	$\Delta\nu_{1/2}$ (Hz)
176.12	C=O (GlcNAc)	2.680	0.7	21.22
175.44	C=O (GlcA)	3.565	0.7	26.05
170.19	$C{=}O_{cr.link.}$ (GlcA)	1.780	0.7	51.26
104.19	$C_{1'}$ (GlcA)	0.064	1.8	53.23
101.64	C_1 (GlcNAc)	0.058	1.7	64.70
83.47	C_3 (GlcNAc)	0.057	1.6	60.29
81.24	$C_{4'}$ (GlcA)	0.055	1.6	43.25
77.39	$C_{5'}$ (GlcA)	0.070	1.7	35.41
76.61	C_5 (GlcNAc)	0.071	1.7	38.58
74.46	$C_{3'}$ (GlcA)	0.055	1.6	49.89
73.90	$C_{2'}$ (GlcA)	0.068	1.6	31.48
69.45	C_4 (GlcNAc)	0.054	1.7	42.90
61.42	C_6 (GlcNAc)	0.066	1.8	38.26
55.41	C_2 (GlcNAc)	0.054	1.6	39.99

[a] Errors in the relaxation times are less than 5%.

Table 5. Evaluation of the crosslinking degree of the four hydrogels using different analytical techniques

	Degree of crosslinking (%)		
	NMR	POT.TIT	Theor (CMP-I)
Hyal-1,3-DAP	43.9 ± 3.1	48.0 ± 2.0	50
HyalS-1,3-DAP	46.3 ± 3.1	48.0 ± 2.0	50
Hyal-1,6-DAE	44.5 ± 3.1	45.0 ± 3.0	50
HyalS-1,6-DAE	43.1 ± 3.1	45.0 ± 3.0	50

the decrease in mobility. This effect is partially counteracted by the high water content, due to the chemical nature and the number of substituents of the polymer and to the groups involved in the crosslinking. In fact, the groups are able to strongly interact with water and to enhance the low mobility due to the presence of crosslinking and to eventual entanglements of the polymeric chains near the crosslinking sites. The situation is consequently different from the dissolved polymer chains in which the groups undergo rapid molecular tumbling and internal rotations.

The ^{13}C NMR T_1, T_2 derived from $\Delta\nu_{1/2}$ and NOE data cannot be explained by a single rotational correlation time because of fast bond oscillations or local conformational changes and rotation of the whole chain due to much slower modes, which all take place even in crosslinked polymers. All of our data require a distribution of correlation times for dipolar relaxation of the ^{13}C nuclei. Several methods are available for the calculation of distribution of correlation times in polymers,[28–30] but we chose to discuss our results only qualitatively,[31] as crosslinking causes low frequency motions in the polymers. In fact, τ_c values in the range 10^{-9}–10^{-10} s can be calculated. Hyal-1,3-DAP and HyalS-1,3-DAP exhibit very similar T_1 and T_2 values, lower than Hyal-1,6-DAE and HyalS-1,6-DAE.

2.5. Low-resolution NMR

The hyaluronan-based hydrogel samples studied by low-resolution NMR spectroscopy and their equilibrium water contents (as percentages of the total weight) are reported in Table 6. Similar results were obtained by measuring the water content (W.C.) of all the hydrogels with the following formula:

$$\text{W.C.} = [(W_s - W_d)/W_s] \times 100$$

where W_s and W_d are the weight of the swollen and dried hydrogels, respectively.[32] The water up-take measurements were performed as reported in Experimental and shown in Table 6. The swelling degree values obtained for crosslinked Hyal-1,3 and Hyal-1,6 showed no large differences, and no significant changes were observed between crosslinked HyalS-1,3 and HyalS-1,6. The results also highlighted the role of negative charges in increasing the swelling degree of all the hydrogels.[18]

Different values of water proton NMR relaxation times can be measured in heterogeneous systems, as in hydrogels, due to the presence of different components, and different compartments, that is, gel meshes or junction zones. Furthermore, water relaxation is affected by the polymer network structure as a result of water-macromolecule interactions. Not only do translation and rotation of water molecules affect relaxation, but the chemical exchange process between water molecules

Table 6. Water contents of the crosslinked hyaluronan hydrogels determined by NMR and by weighing

Sample	$\%_{w/w}$ H_2O (NMR)	$\%_{w/w}$ H_2O (Weighing)
Hyal-1,3-DAP	96 ± 3	98.0 ± 1.0
HyalS-1,3-DAP	90 ± 5	99.0 ± 0.5
Hyal-1,6-DAE	97 ± 2	98.0 ± 1.0
HyalS-1,6-DAE	97 ± 2	99.0 ± 0.5

Table 7. Transverse relaxation times and signal percentages of the two components of water in crosslinked hyaluronan hydrogels at 310 K

Sample	Bulk water		Meshes water	
	%	T_2 (s)	%	T_2 (s)
Hyal-1,3-DAP	95.1 ± 0.2	0.994 ± 0.004	4.9 ± 0.1	0.147 ± 0.009
HyalS-1,3-DAP	84.0 ± 0.3	0.646 ± 0.002	16.0 ± 0.3	0.058 ± 0.002
Hyal-1,6-DAE	80.5 ± 0.1	1.016 ± 0.004	19.5 ± 0.3	0.102 ± 0.001
HyalS-1,6-DAE	58.5 ± 0.1	0.522 ± 0.003	41.5 ± 0.1	0.071 ± 0.008

and polymers or other solutes also strongly contributes to T_1 and T_2 values. Several pieces of compositional and structural information, as well as modifications of the hydrogel structure, can thus be detected by analysis of the water proton relaxation curves.

The relaxation curves in general, and decay magnetisation curves in particular, show multi-exponential behaviour in hydrogels.[33–36] As may be expected, the transverse relaxation curves of water in our hydrogels showed biexponential behaviour, because of the presence of different components in the samples. In fact, water can spread into the space between the meshes ('bulk water') and within the meshes. Water can be seen as an integral part of the polymer structure or as trapped within interstitial spaces. In general, different water types are in mutual diffusive exchange; if the water diffusion is sufficiently slow compared to the relaxation time, the relaxation is in the 'slow diffusive exchange' regime and multi-component relaxation is observed.[35] Table 7 summarises the values obtained for transverse relaxation times measured at 310 K for both components of water in the four types of hydrogels.

It is immediately evident that the T_2 values of both components are lower than those of pure water (about 2 s at the same temperature), indicating an interaction between water and macromolecular network. The component with longer T_2 was ascribed to water molecules remote from the polymer network. Their motion is slightly affected by the polymer presence and therefore called 'bulk water'. Generally, the reduced T_2 of bulk water can be simply explained as being due to the anisotropic motion that water molecules can undergo in a restricted region, with possible further lowering due to proton exchange with polymer exchangeable protons.

The fast relaxing component ('meshes water') was attributed to the water molecules within the interstitial spaces of the polymer. Its transverse relaxation time is further reduced by a factor ranging from 6 and 10. This result is often encountered when dealing with water relaxation in gels and other heterogeneous systems.[35–38] The behaviour is generally explained by a slowing down of the rotational motion of water molecules, the degree of reduction being related to the strength of the interaction with the macromolecular network. The chemical exchange mechanism is also expected to play a major role in such reductions.

Our model does not imply the concept of 'bound water' for the assignment of the different components in the water relaxation curve in hyaluronan-based hydrogel samples. In fact, the different T_2 values for the two types of water molecules can be affected by chemical and diffusive exchange contributes between water and the polymer network. Variations in water T_2 values can therefore be used to monitor changes in the structure of hyaluronan-based hydrogel samples.

The T_2 values of bulk water in Hyal-1,3-DAP and Hyal-1,6-DAE, which are higher than in their sulfated derivatives, can be explained by the presence of a lower number of exchangeable hydrogens on these macromolecules, because the swelling percentages did not suggest a larger-meshed net (i.e., a larger free volume for water). The lower T_2 values (coupled with higher signal percentage values) for meshes water in sulfated hydrogels provide at least qualitative evidence for lower mobility of polymer chains, and hence a higher degree of organisation of sulfated hydrogels with respect to the equivalent native ones. Furthermore, the lowest T_2 value found for HyalS-1,6-DAE can be explained by the high repulsion among the chains due to the presence of negative charged groups bonded to an aliphatic chain. This produces the well-known 'stiffening effect'[39] in HyalS-1,6-DAE, as revealed by the T_2 value. This phenomenon is also confirmed by the high percentage of meshes water. In fact, as shown in Table 7, only HyalS-1,6-DAE showed very similar percentages of bulk and meshes water. This situation suggests that water molecules tend to organise themselves to minimise contact with the hydrophobic environment due to repulsion among the chains. This effect is obviously minimal in HyalS-1,3-DAP due to its very short aliphatic chain, so in this case most of the water molecules are free to move similarly to non-sulfated hydrogels.

With the exception of HyalS-1,6-DAE, analysis of the longitudinal magnetisation curve measured for the hydrogels gave a single component (Table 8). The T_1 value of water molecules and the high water percentage of the meshes in HyalS-1,6-DAE confirm the stiffening effect observed by the T_2 measurements. In fact, although the T_1 value is generally less sensitive than T_2 to the different type of water molecule, it is possible to differentiate the two water types in HyalS-1,6-DAE due to the high degree of organisation.

Table 8. Longitudinal relaxation times of the water in crosslinked hyaluronan hydrogels at 310 K

Sample	T_1 (s)
Hyal-1,3-DAP	2.36 ± 0.01
HyalS-1,6-DAP	1.77 ± 0.02
Hyal-1,6-DAE	2.70 ± 0.02

	Bulk water		Meshes water	
	%	T_1 (s)	%	T_1 (s)
HyalS-1,6-DAE	63.4 ± 0.6	1.28 ± 0.06	36.6 ± 0.6	0.21 ± 0.02

For the HyalS-1,6-DAE sample the relaxation time and signal percentage values of the two components are reported.

The T_1/T_2 ratio values reported in Table 9 provide evidence for anisotropy of molecular motions of the bulk water molecules and the water in the meshes of HyalS-1,6-DAE. In fact, a situation of isotropic motion with only one correlation time (τ_c) is characterised by a T_1/T_2 value between 1 and 1.6; the T_1/T_2 ratio increases with any deviations from isotropic motion and/or due to the distribution of τ_c.[34,40] This is in agreement with the description of water molecules confined in gel meshes whose motion is affected by chemical exchanges with polymers, while it is in contrast with the idea of bulk water molecules that are free to rotate/translate, as in a solution. This confirms that the reduction of bulk water relaxation times is due to the anisotropic motions in a restricted region rather than to the chemical exchange as in the meshes. For the latter molecules, the rotation may be affected by interaction with the polymer and can be described by different correlation times, according to a previously developed model.[41]

The self-diffusion coefficients D were measured by the pulsed field gradient spin echo (PFG SE) sequence to characterise the water mobility inside the hydrogels. The results obtained are reported in Table 10. Water self-diffusion coefficients in such systems are slightly slower than in pure water at the same temperature ($D_{water}^{310\,K} = 2.92 \times 10^{-9}$ m^2 s^{-1}). In addition, the echo attenuation curves were monoexponential in all cases, thus excluding contribution from other diffusing species and the presence of barriers to the translational motion of water molecules in the echo time of the PFG NMR experiment (i.e., over a distance of up to a few micrometers). In fact, by the Einstein equation $\langle z^2 \rangle = 2Dt$ (where $t = (\Delta - \delta/3)$ is the echo time of the PFG SE experiment), the minimum amplitude for diffusional domains can be derived (38 μm for Hyal-1,3-DAP; 39 μm for HyalS-1,6-DAP; 41 μm for Hyal-1,6-DAE; and 40 μm for HyalS-1,6-DAE), so that restricted diffusion under these distances can be excluded.[35,41,42] Therefore no significant differences were founds in terms of transport properties of the four hyaluronan-based hydrogels.

Table 9. T_1/T_2 ratio values of the water in crosslinked hyaluronan hydrogels at 310 K

Sample	T_1/T_2 bulk water	T_1/T_2 meshes water
Hyal-1,3-DAP	2.37 ± 0.02	—
HyalS-1,6-DAP	3.00 ± 1.00	—
Hyal-1,6-DAE	2.66 ± 0.03	—
HyalS-1,6-DAE.	2.40 ± 0.10	2.9 ± 0.6

Table 10. Water self-diffusion coefficients measured at 310 K by PFG SE

Sample	D (10^{-9} m^2 s^{-1})
Hyal-1,3-DAP	2.43 ± 0.04
HyalS-1,6-DAP	2.57 ± 0.03
Hyal-1,6-DAE	2.82 ± 0.03
HyalS-1,6-DAE	2.66 ± 0.06

The low-resolution NMR measurements highlighted that the reaction developed makes it possible to obtain a homogeneous structure with reproducible meshes whose dimension, being similar for all the hydrogels, is dependent only on the procedure for synthesis or the amount of activating agent (CMP-I) added. In fact, the T_1/T_2 ratio, which provides a measure of the system isotropy, shows that the anisotropy is not as high as it would be if the crosslinkings were not homogenously distributed.

The excellent biocompatibility of these materials is further confirmed by the high water content, determined by low-resolution NMR data. Moreover, the rates at which water diffuses into the meshes and between the meshes and the data derived on the size of the meshes confirm the positive properties of these polymers in drug release[43] and in cell adhesion.[44]

3. Experimental

3.1. Materials

The hyaluronic acid sodium salt (Hyal, molecular weight 200 kD) was supplied by Fidia S.p.A. (Abano Terme, Padova, Italy). 1,3-Diaminopropane (DAP), 1,6-diaminohexane (DAE), *N*,*N*′-dimethylformamide (DMF), 2-chloro-1-methylpyridinium iodide (CMP-I), tetrabutylammonium hydroxide, Et_3N, EtOH and all other reagents were purchased from Fluka Chemie AG (Switzerland).

3.2. Hydrogel synthesis and characterisation

The hyaluronan-based 50% hydrogels were synthesised as previously described.[18] Briefly, a solution of polysaccharide sodium salt (1.0% w/v) was subjected to a sodium–hydrogen ion exchange using Dowex 50WX8 resin and was then added to a 5% tetrabutylammonium hydroxide solution until a pH of 8–9 was reached. The

solution was then lyophilised, obtaining the tetrabutylammonium (TBA) salt of the polysaccharide. The TBA salt was dissolved in DMF under stirring and nitrogen flow. The solution was kept at 0 °C until the activating agent CMP-I was added. The amount of CMP-I added depended on the quantity of carboxylate groups to be activated (50%). 1,3-Diaminopropane and 1,6-diaminohexane were used as crosslinking agents. The reaction was catalysed by a small amount of Et_3N as an HI scavenger. The reaction was left at rt for 3–4 h. The hydrogel formed was washed alternately with doubly distilled H_2O and EtOH until no more solvents or secondary products were found in the washing solution, as demonstrated by UV absorption measurements. The ninhydrin assay was performed to check for the presence of unreacted NH_2 groups of the alkylic diamines used as crosslinkers.[45] A small amount of dried hydrogel was rinsed with 1 mL of acetate buffer (pH 5) and a small amount of ninhydrin was added. The mixture was left in boiling water for 15 min, then 15 mL of 50% EtOH was added and protected from direct exposure to light for 1 h. The colour of the mixture becomes violet in the presence of free amine groups.

3.3. Sulfation of 50% hydrogels

Sulfation of the materials was achieved by immersing the already crosslinked 50% hydrogels in DMF under mechanical stirring at rt. The sulfating agent (sulfur trioxide–pyridine complex, SO_3–Py) in a molar ratio of 1:2 with the sulfatable groups (OH) of the polysaccharide was dissolved in the minimum amount of DMF and the resulting solution was added to the hydrogel. The reaction was maintained under nitrogen flow for 2 h and was then stopped by adding doubly distilled water and sodium hydroxide 1 M up to pH 9. The sulfated hydrogels were then washed with 95% EtOH and H_2O until no secondary products were found in the washing solutions. The number of sulfate groups (mol SO_3^- per mg of dry hydrogel) was established by the 'toluidine blue' method:[46] an exact amount of dry hydrogel was weighed and immersed in an exact volume of toluidine blue solution whose absorbance had been measured previously; the decrease of absorbance was recorded by UV spectrometer (Pharmacia, Biochrom 4060), and the number of sulfate groups was calculated using a calibration curve recorded at a wavelength of 560 nm. The calibration curve was obtained by dissolving different amounts of HyalS polymer, for which the number of sulfate groups was established previously by elemental analysis.

3.4. Potentiometric titration

Potentiometric titration was carried out to verify the number of carboxylate groups of the polysaccharide involved in the crosslinking reaction. The dried hydrogels (20 mg) were finely dispersed in a thermostatic glass cell at 25 °C, at a constant ionic strength of 0.1 M NaCl with a known amount of 0.1 M HCl (2 mL). Titration was then performed with 0.1 M NaOH (3 mL) and back titration with 0.1 M HCl. The experimental conditions involved a stabilisation time of 360 min for the initial system and a delay time of 21 min between each addition of titrant. The titration data were collected by a Crison MicropH-2002, equipped with a combined electrode (mod.6.0204.000), together with an automatic Crison microburette (mod.3031), connected to a PC.

3.5. FTIR-ATR analysis

ATR spectra of the samples in dry form were recorded on a Bio-rad FTS6000 between 4000 and 750 cm^{-1} following the classic procedure.[47] An MCT (mercury–cadmium–tellurium) detector was used and the apparatus was purged with nitrogen. As previously experienced, we averaged 50 scans at a resolution of 1.0 cm^{-1}. The frequency scale was internally calibrated with a helium–neon reference laser to an accuracy of 0.01 cm^{-1}.

3.6. High-resolution NMR

The high-resolution NMR spectra were measured on a Bruker AM 500 spectrometer operating at 500.13 MHz for proton and at 125.37 MHz for ^{13}C. The fully proton decoupled high-resolution ^{13}C spectra were performed on hydrogels swollen in deuterium oxide (ISOTEC INC., 99.96% purity) at the controlled temperature of 310 ± 1 K. Spectra were obtained with a 5 mm dual probe using proton broadband decoupling of 3.5 kHz, a spectral width of 30,000 Hz, a pulse length of 9.5 μs for the $\pi/2$ pulse, a relaxation delay of 9.5 s, an acquisition time of 0.5 s, and 2000 scans. Spectra were referenced to TSP (trimethylsilyl-d_4-propionate). The ^{13}C dynamic parameters were calculated as follows. The spin–lattice relaxation times (T_1) were measured by the standard inversion recovery pulse sequence (π-τ-$\pi/2$-acq) present in the instrumental routine. A repetition time of at least $5 \times T_1$ (of the slowest relaxating carbon atom in the sample) was used. A total of 15 experiments were performed with varying τ-values. Data were processed using WINNMR software (Bruker Spectrospin s.r.l.—Italia) and exponential regressions were computed using NONLIN software (version 3.0). The NOE was measured using the inverse gated decoupling sequence.

3.7. Low-resolution NMR

Samples were prepared for low-resolution NMR measurements by swelling an exact amount of the different

crosslinked hyaluronans with distilled H_2O in a 10 mm NMR tube for 24 h at 310 ± 1 K. The equilibrium H_2O contents are reported in Table 7. Experiments were performed on a Minispec PC120 pulsed NMR spectrometer with an operating frequency of 20 MHz for protons (magnetic field strength: 0.47 T). The NMR spectrometer was equipped with a pulsed gradient unit. Before NMR measurements, a sample tube was placed into the NMR probe as long as needed to reach thermal equilibration (90 min). The measurements were performed at a temperature of 310 ± 1 K. The longitudinal relaxation times (T_1) were determined by the standard inversion recovery (IR) sequence.[48] The relaxation recovery curves were fitted using NONLIN software (version 3.0). The transverse relaxation times (T_2) were measured using the Carr–Purcell–Meiboom–Gill (CPMG) sequence.[49] The decay of the transverse magnetisation was found to be constantly biexponential; the amplitudes and the spin–spin relaxation time of the two components were calculated by means of nonlinear least-squares data fitting with a home-written computer program based on the Marquardt algorithm.[50]

Water self-diffusion coefficient measurements were carried out using the standard pulsed field gradient spin echo (PFG SE) sequence.[51] Keeping the gradient amplitude G fixed, the amplitude of the NMR signal at a fixed echo time (A_G) is given by

$$A_G = A_0 \exp(-kD)$$

where A_0 is the echo amplitude in the absence of the pulsed gradients, and k is given by $k = (\gamma\delta G)^2(\Delta - \delta/3)$ (γ is the proton magnetogyric ratio, and Δ is the time interval between the two gradient pulses of duration δ). D values were determined by a monoexponential fitting of the echo amplitudes measured at different Δ values.

Acknowledgements

The authors gratefully acknowledge financial support from the Italian Ministry of Education, University and Research (PRIN 2003 project 2003099430).

References

1. Flatau, A. B.; Chong, K. P. *Eng. Struct.* **2002**, *24*, 261–271.
2. Takagi, T. *Mater. Sci. Eng.* **1998**, *A253*, 30–41.
3. Miyata, T.; Uragami, T.; Nakamae, K. *Adv. Drug Delivery Rev.* **2002**, *54*, 79–98.
4. Gehrke, S. H.; Lee, P. I. In *Specialised Drug Delivery System*; Marcel Dekker: New York, 1990.
5. Mamytbekov, G.; Bouchal, K.; Ilavsky, M. *Eur. Polym. J.* **1999**, *35*, 1925–1933.
6. Bajpa, A. K.; Giri, A. *Carbohydr. Polym.* **2003**, *53*, 271–279.
7. Qu, X.; Wirsen, A.; Albertsson, A. C. *Polymer* **2000**, *41*, 4589–4598.
8. Barbucci, R.; Magnani, A.; Rappuoli, R.; Lamponi, S.; Consumi, M. *J. Inorg. Biochem.* **2000**, *79*, 119–125.
9. Barbucci, R.; Leone, G.; Magnani, A.; Montanaro, L.; Arciola, C. R.; Peluso, G.; Petillo, O. *J. Mater. Chem.* **2002**, *12*, 3084–3092.
10. Jansen, K.; van der Werff, J. F. A.; van Wachem, P. B.; Nicolai, J. P. A.; de Leij, L. F. M. H.; van Luyn, M. J. A. *Biomaterials* **2004**, *25*, 483–489.
11. Suh, J. K. F.; Matthew, H. W. T. *Biomaterials* **2000**, *21*, 2589–2598.
12. Rowley, J. A.; Madlambayan, G.; Mooney, D. J. *Biomaterials* **1999**, *20*, 45–53.
13. Nitschke, M.; Zschoche, S.; Baier, A.; Simon, F.; Werner, C. *Surf. Coat. Technol.* **2004**, *185*, 120–125.
14. Topez, M.; Mutaz, B. *Oper. Tech. Plastic Reconstr. Surg.* **2003**, *9*, 79–81.
15. Manna, F.; Dentini, M.; Desideri, P.; De Pità, O.; Mortella, E.; Maras, B. *J. Eur. Acad. Dermatol. Venereol.* **1999**, *13, 183–192.*
16. Barbucci, R.; Leone, G.; Lamponi, S. *J. Biomed. Mater. Res., Part B. Appl.* **2006**, *76B*, 33–40.
17. Barbucci, R.; Magnani, A.; Leone, G. *Polymer* **2002**, *43*, 3541–3548.
18. Barbucci, R.; Rappuoli, R.; Borzacchiello, A.; Ambrosio, L. *J. Biomater. Sci., Polym. Ed.* **2000**, *11*, 383–399.
19. Bellamy, L. J. *The Infrared Spectra of Complex Molecules*, 3rd ed.; Chapman and Hall: New York, 1980.
20. Livant, P.; Roden, L.; Rama Krishna, N. *Carbohydr. Res.* **1992**, *237*, 271–281.
21. Cavalieri, F.; Chiessi, E.; Paci, M.; Paradossi, G.; Flaibani, A.; Cesaro, A. *Macromolecules* **2001**, *34*, 99–109.
22. Dais, P.; Tylianakis, E.; Kanetakis, J.; Taravel, F. R. *Biomacromolecules* **2005**, *6*, 1397–1404.
23. Segre, A. L.; Delfini, M.; Paci, M.; Raspolli-Galletti, A. M.; Solaro, R. *Macromolecules* **1985**, *18*, 44–48.
24. Murase, N.; Watanabe, T. *Magn. Reson. Med.* **1989**, *9*, 1–7.
25. Dais, P. *Adv. Carbohydr. Chem. Biochem.* **1995**, *51*, 63–131.
26. Miura, N.; Shioya, S.; Kurita, D.; Shigematsu, T.; Mashimo, S. *Am. J. Physiol. Lung Cell Mol. Physiol.* **1999**, *276*, 207–212.
27. Cowman, M. K.; Feder-Davis, J.; Hittner, D. M. *Macromolecules* **2001**, *34*, 110–115.
28. Shaefer, G.; Natusch, D. F. S. *Macromolecules* **1973**, *5*, 416–427.
29. Ford, W. T.; Balakrishnan, T. *Macromolecules* **1981**, *14*, 284–288.
30. Petit, J. M.; Zhu, X. X. *Macromolecules* **1996**, *29*, 2075–2081.
31. Doddrell, D.; Allherand, A. *J. Am. Chem. Soc.* **1971**, *93*, 1558–1559.
32. Barbucci, R.; Magnani, A.; Consumi, M. *Macromolecule* **2000**, *33*, 7475–7480.
33. Hills, B. P.; Belton, P. S.; Quantin, V. M. *Mol. Phys.* **1993**, *78*, 893–908.
34. Belton, P. S. *Int. J. Biol. Macromol.* **1997**, *21*, 81–88.
35. Barbieri, R.; Quaglia, M.; Delfini, M.; Brosio, E. *Polymer* **1998**, *39*, 1059–1066.
36. Brosio, E.; Barbieri, R.; Gianferri, R. In *Recent Research Developments in Polymer Science*; Pandalai, S. G., Ed.; Transworld Research Network: Kerala, India, 2002.
37. Belton, P. S.; Hills, B. P. *Mol. Phys.* **1987**, *61*, 999–1018.
38. Hills, B. P.; Wright, K. M.; Belton, P. S. *Mol. Phys.* **1989**, *67*, 1309–1326.
39. Garbi, S.; Afli, A.; Garbi, R. E.; Gandini, A. *Polym. Int.* **2001**, *50*, 509–514.

40. Brosio, E.; D'Ubaldo, A.; Carnevale, E.; Giusti, A. M. *Cell. Mol. Biol.* **1993**, *39*, 199–204.
41. Halle, B.; Anderson, T.; Forsen, S.; Lindman, B. *J. Am. Chem. Soc.* **1981**, *103*, 500–508.
42. Callaghan, P. T.; Jolley, K. W.; Lelièvre, J. *Biophys. J.* **1979**, *28*, 133–142.
43. Barbucci, R.; Fini, M.; Martini, L.; Torricelli, P.; Giardino, R.; Lamponi, S.; Leone, G. *J. Biomed. Mater. Res., Part B* **2005**, *75B*, 42–48.
44. Barbucci, R.; Leone, G.; Lamponi, S. *J. Biomed. Mater. Res. Part B: Appl. Biomater.* **2006**, *76B*, 33–40.
45. Virender, K. S.; Kent, S. B. H.; Tam, J. P.; Merrifield, R. B. *Anal. Biochem.* **1981**, *117*, 147–157.
46. Smith, P. K.; Mallia, A. K.; Hermanson, G. T. *Anal. Biochem.* **1980**, *109*, 466–473.
47. Koenig, J. L. *Spectroscopy of Polymers*; American Chemical Society: Washington, DC, 1992.
48. Ernst, R. R.; Bosedhausen, G.; Wokaun, A. *Principles of Nuclear Magnetic Resonances in One and Two Dimensions*; Oxford Clarendon Press: New York, NY, 1991.
49. Meiboom, S.; Gill, D. *Rev. Sci. Instrum.* **1958**, *29*, 688–691.
50. Marqardt, D. W. *J. Soc. Ind. Appl. Math.* **1963**, *11*, 431–441.
51. Stejskal, E. O.; Tanner, J. E. *J. Chem. Phys.* **1965**, *42*, 288–292.